DESIGN OF A CONTROL LAW FOR A MAGNETO-RHEOLOGICAL SUSPENSION

Alessandro Giua, Mauro Melas, Carla Seatzu

Department of Electrical and Electronic Engineering, University of Cagliari, Italy
fax: +39-070-675-5782
e-mail: {giua,seatzu}@diee.unica.it.

Keywords: Semi-active suspension, magneto-rheological damper, linear quadratic regulator, vehicle dynamics.

Abstract

In this paper we present a design procedure for semiactive suspensions of road vehicles, where the shock absorber (damper) uses magneto-rheological fluid instead of oil. We first derive a target active control law that minimizes a quadratic performance index and takes the form of a feedback control law. Then, we approximate the target law by controlling the damper coefficient f of the semiactive suspension. The nonlinear characteristics force-velocity of the damper are used to approximate the target law. To improve the efficiency of the proposed system, we take into account the updating frequency of the coefficient f and compute the expected value of f using a predictive procedure.

1 Introduction

In this paper we apply a procedure for the design of a semiactive suspension to the case of a suspension for road vehicles with a magneto-rheological damper.

In a fully active suspension there are no passive elements, such as dampers and springs. The interaction between vehicle body and wheel is regulated by an actuator of variable length. The actuator is usually hydraulically controlled and applies between body and wheel a force that represents the control action generally determined with an optimization procedure.

Active suspensions [3, 8, 14] have better performance than passive suspensions with regard to comfort, road holding, and rideability. However, active suspension systems are rather complex, since they require several components such as actuators, servovalves, high-pressure tanks for the control fluid, either sensors for detecting the system state or appropriate system state observers, etc. Moreover, the associated power, that must be provided by the vehicle engine, may reach the order of several 10 KW depending on the required performance. Thus, these suspension systems have a very high cost.

As a viable alternative to a purely active suspension system, the use of semiactive suspensions has been considered [1, 7, 9, 13]. A semiactive suspension consists of a spring and a damper but, unlike a passive suspension, the value of the damper coefficient f can be controlled and updated. In some type of suspensions, but this case is not considered here, it may also be possible to control the elastic constant of the spring.

A semiactive suspension is a valid engineering solution when it can reasonably approximate the performance of the active control. In fact, a semiactive suspension requires a low power controller that can be easily realized at a lower cost than that of a fully active one. In general, a semiactive suspension design consists of two phases: (a) design a good active law, $u_t(\cdot)$ to be considered as a "target"; (b) choose at time t a suitable value of the damper coefficient $f(t)$ so that the control force $u_s(\cdot)$ generated by the suspension system approximates as close as possible the target law $u_t(\cdot)$.

In this paper the semiactive suspension system is designed using a shock absorber that uses magneto-rheological (MR) fluid instead of oil. The magneto-rheological response of MR fluids results from the polarization induced in suspended particles by the application of an external field. This system presents several advantages with respect to more conventional systems: it has no moving parts other than the piston and rod itself; the required power is very low, and the reaction time is very fast.

A real damper, as well as the magneto-rheological one, exhibits a nonlinear behavior that can be described through a family of nonlinear characteristics force-velocity, parameterized by constant current values. These characteristics are used to approximate the target active law.

In the following we discuss in detail the two main phases involved in the design of the semiactive suspension system.

Target active law

Thompson [14] was the first to explore the use of optimal control techniques to design an active law so as to minimize a performance index of the form $J = \int_0^\infty (\boldsymbol{x}^T(t)\boldsymbol{Q}\boldsymbol{x}(t) + ru^2(t))dt$, where $\boldsymbol{x}(t)$ is the system state and $u(t)$ the control force provided by the actuator at the time instant t. This design technique is called LQR [12] and has been used by many authors. Its two main advantages are: a) the optimal solution can be easily computed solving an algebraic Riccati equation; b) it takes the form of a state feedback law with constant gains, i.e., $u(t) = -\boldsymbol{K}\boldsymbol{x}(t)$. Note, however, that in most cases the system state is not directly accessible or measuring it is too expensive. Thus, an asymptotic state observer needs to be used. This implies that the real control law takes the form $u_t(t) = -\boldsymbol{K}\hat{\boldsymbol{x}}(t)$ where $\hat{\boldsymbol{x}}(t)$ denotes the system state estimate at the generic time instant t.

In this paper we consider an original procedure for the design of an asymptotic state observer firstly proposed by the authors in [5]. Such a procedure well fits within the present application whose main requirement is that of reconstructing the system state when external disturbances are acting on it, while the initial state may always be assumed known.

Semiactive approximation

On the base of the previous analysis, we propose to choose as target for the semiactive control law $u_s(\cdot)$ the law $u_t(\cdot)$. Every Δt time units the controller should select on the base of the current value of the suspension velocity, the new damper coefficient f using the nonlinear characteristics force-velocity of the damper. The new value of f is chosen so as to minimize the quadratic difference among the semiactive and the target active control force. The value of Δt cannot be chosen arbitrarily,

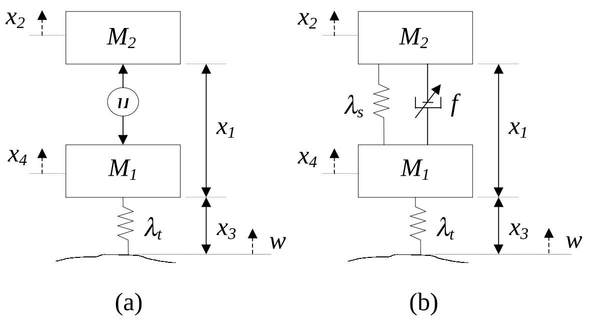

Figure 1: Scheme of two degree-of-freedom suspension: (a) active suspension; (b) semiactive suspension.

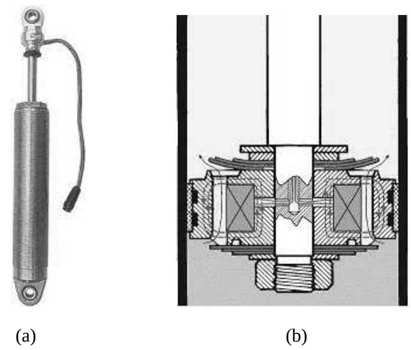

Figure 2: The *CARRERA*^{TM} *MagnetoShock*^{TM} (a) and a scheme of its internal structure (b).

but its lower bound is imposed by the physical limits on the updating frequency of the damper coefficient f. In the case of the MR damper the updating frequency may take values of the order of 500 Hz.

In this paper we improve the efficiency of the resulting suspension system taking into account the time Δt required to update f. More precisely, the new value of f at the generic time instant t is selected so as to minimize the quadratic difference $(u_t(t+\Delta t) - u_s(t+\Delta t))^2$. In such a way, as proved via various numerical simulations, we are able to compensate the delay on the updating of f, thus producing a significant improvement on the system behavior, that is evaluated in terms of the performance index J [11].

Note that this approach has been possible thanks to the efficiency of the proposed state observer [5] that also provides a good estimate of the system state derivatives.

Different simulations have been carried out, considering the effect of input disturbances caused by the road profile and the effect of non–null initial conditions on the state. The results of these simulations show that the semiactive suspension performs reasonably well, and is a good approximation of the target active suspension, while it introduces significant improvements with respect to a completely passive suspension [4]. Note that in all numerical simulations we considered a real existing damper, the *CARRERA*^{TM} *MagnetoShock*^{TM}, whose physical characteristics are reported in the CARRERA web site [2]. The main drawback of this damper, according to the simulation results shown in section 5, is not due to the updating frequency (that does not pose in practice any limitation) but lies in the fact that even with a null magnetic field the damper coefficient is often too high.

2 Dynamical model of the suspension system

Let us now consider the completely active suspension system with two degrees of freedom schematized in Figure 1.a. We used the following notation: M_1 is the equivalent unsprung mass consisting of the wheel and its moving parts; M_2 is the sprung mass, i.e., the part of the whole body mass and the load mass pertaining to only one wheel; λ_t is the elastic constant of the tire, whose damping characteristics have been neglected. The state component $x_1(t)$ is the deformation of the suspension with respect to (wrt) the static equilibrium configuration, taken as positive when elongating; $x_2(t)$ is the vertical absolute velocity of the sprung mass M_2; $x_3(t)$ is the deformation of the tire wrt the static equilibrium configuration, taken as positive when elongating (under the assumption of flat road surface, this is also the deformation of the tire); $x_4(t)$ is the vertical absolute velocity of the unsprung mass M_1; $u(t)$ is the control force produced by the actuator; $w(t)$ is the function representing the disturbance. It coincides with the absolute vertical velocity of the point of contact of the tire with the road.

It is readily shown that the state variable mathematical model of the system under study is given by [3]

$$\dot{\boldsymbol{x}}(t) = \boldsymbol{A}\boldsymbol{x}(t) + \boldsymbol{B}u(t) + \boldsymbol{L}w(t) \tag{1}$$

where $\boldsymbol{x}(t) = [x_1(t),\ x_2(t),\ x_3(t),\ x_4(t)]^T$ is the state, whereas the constant matrices $\boldsymbol{A}$, $\boldsymbol{B}$ and $\boldsymbol{L}$ have the following structure:

$$\boldsymbol{A} = \begin{bmatrix} 0 & 1 & 0 & -1 \\ 0 & 0 & 0 & 0 \\ 0 & 0 & 0 & 1 \\ 0 & 0 & -\lambda_t/M_1 & 0 \end{bmatrix}, \quad \boldsymbol{B} = \begin{bmatrix} 0 \\ 1/M_2 \\ 0 \\ -1/M_1 \end{bmatrix},$$

$$\boldsymbol{L} = [\ 0 \quad 0 \quad -1 \quad 0\ ]^T.$$

Now, let us consider Figure 1.b that represents a conventional semiactive suspension composed of a spring, whose characteristics force-deformation is nonlinear, and a damper with adaptive characteristic coefficient $f = f(t)$.

The effect of this suspension is equivalent to that of a control force $u_s(t) = -[\lambda_s\ f(t)\ 0\ -f(t)]\boldsymbol{x}(t)$.

Note that, as f may vary so as to best approximate the active control force, $u_s(t)$ is both a function of f and of $\boldsymbol{x}(t)$. It is immediate to verify that the state variable mathematical model of the semiactive suspension is still given by equation (1) where $u(t)$ is replaced by $u_s(t)$.

3 The magneto-rheological damper

In this paper we consider a shock absorber (damper) that uses Magneto-Rheological (MR) fluid instead of oil. In particular, we refer to a real existing damper shown in Figure 2.a, the *CARRERA*^{TM} *MagnetoShock*^{TM}, whose physical characteristics are given in [2].

The MR fluid is basically composed of micron sized particles of iron suspended in an oil base. The magnetorheological response of MR fluids results from the polarization induced in suspended particles by the application of an external field. The interaction between the resulting induced bipoles causes the particles to form columnar structures, parallel to the applied field. These chain-like structures restrict the motion of

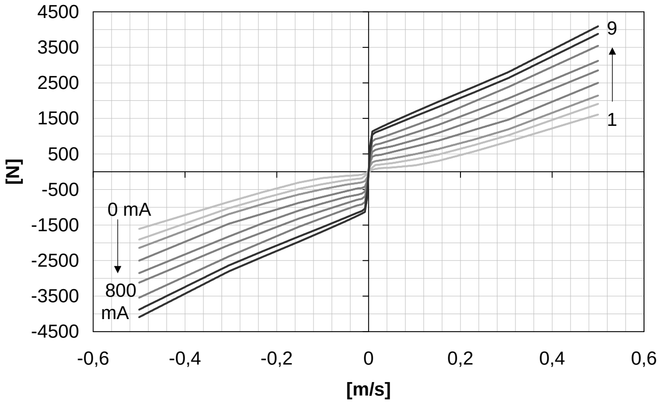

Figure 3: The nonlinear characteristics of the MR damper.

the fluid, thereby increasing the viscous characteristics of the suspension. The mechanical energy needed to yield the microstructure increases as the applied field increases resulting in a field dependent yield stress. In the absence of an applied field, MR fluids exhibit Newtonian-like behavior [10].

The internal structure of the damper is sketched in Figure 2.b. The piston contains an annular orifice, through which the MR fluid passes, and an electromagnet. The controller varies the magnetic field of the electromagnet and the damping force varies proportionally. The MagnetoShock^{TM} has no moving parts (like valves, spring, etc.) other than the piston and rod itself.

The power required is very low (on the average, 3 W per shock) and the reaction time is very fast, usually less than 2 milliseconds. In its simplest form the damping force of the shock can be easily adjusted. It is capable of updating the damping force 500 times/second to each shock.

Figure 3 shows the nonlinear (static) characteristics force-velocity of the considered damper at different constant current values (in this figure, following a usual convention, a positive force corresponds to a positive velocity of deformation).

As we have anticipated in the introduction, on the basis of the simulation results discussed in section 5, the main drawback of this damper is not due to the updating frequency (that does not pose in practice any limitation) but lies in the fact that even with a null magnetic field the damper coefficient is too high. To improve the damper performance it is necessary to have characteristic curves closer to the x axis than the one labelled "1" in Figure 3.

4 Semiactive suspension design

In this section we first discuss how the target active control law has been determined. Then we show how such a control law, that requires an actuator, may be approximated by a semiactive suspension, whose varying parameter is the characteristic coefficient of the damper f.

4.1 Target active control law

The design of the active suspension requires determining a suitable control law $u(\cdot)$ for system (1). To this end, we first determine the control law $u(\cdot)$ that minimizes a performance index of the form

$$J = \int_0^\infty (\boldsymbol{x}^T(t)\boldsymbol{Q}\boldsymbol{x}(t) + ru^2(t))dt$$

where $\boldsymbol{Q}$ is positive semidefinite and $r > 0$. As well known from the literature [12], the solution of this problem can be easily computed by simply solving an algebraic Riccati equation, and takes the form of a feedback control law

$$u(t) = -\boldsymbol{K}\boldsymbol{x}(t).$$

Obviously, when the system state is not directly measured, but is reconstructed via an asymptotic observer, the above control law is replaced by

$$u_t(t) = -\boldsymbol{K}\hat{\boldsymbol{x}}(t)$$

where $\hat{\boldsymbol{x}}(t)$ is the state estimate.

In this paper the asymptotic state observer is designed using the procedure we proposed in [5]. We assume that the suspension and the tire deformation are measurable. This is equivalent to choose

$$\boldsymbol{C} = \begin{bmatrix} 1 & 0 & 0 & 0 \\ 0 & 0 & 1 & 0 \end{bmatrix}$$

for the output equation $\boldsymbol{y}(t) = \boldsymbol{C}\boldsymbol{x}(t)$. This ensures the observability of the pair $(\boldsymbol{A}, \boldsymbol{C})$.

The considered asymptotic state observer has the structure of a Luenberger observer, i.e., it takes the form

$$\dot{\hat{\boldsymbol{x}}}(t) = \boldsymbol{A}\hat{\boldsymbol{x}}(t) + \boldsymbol{B}u(t) + \boldsymbol{K}_0(\boldsymbol{y}(t) - \boldsymbol{C}\hat{\boldsymbol{x}}(t)). \qquad (2)$$

The gain matrix $\boldsymbol{K}_0$ is determined by simply minimizing the H_2 norm of the transfer function matrix

$$\boldsymbol{F}(s) = [s\boldsymbol{I} - (\boldsymbol{A} - \boldsymbol{K}_0\boldsymbol{C})]^{-1}\boldsymbol{L}$$

between the estimate error $\boldsymbol{e}(t) = \boldsymbol{x}(t) - \hat{\boldsymbol{x}}(t)$ and the external disturbance $w(t)$. In such a way we can be sure that we are minimizing the effect of the disturbance on the error estimate.

4.2 Semiactive approximation

In this section we show how the active target control law u_t may be approximated using a MR semiactive suspension, taking into account the nonlinear characteristics force-velocity of the MR damper (see Figure 3). These characteristics are parameterized by the values of the external current (the control action) that enables to modify the viscosity of the fluid and consequently the coefficient of the damper. The aim of the controller is that of selecting the nonlinear characteristic that minimizes the difference among the resulting semiactive control force and the target active control force. The nonlinear characteristic force-deformation of the spring is also taken into account.

Note that a certain time Δt, depending on the physical system, is necessary to update the damper coefficient. In general this time interval also depends on the required variation of the force, and consequently on the required variation of the external current. For small variations of the force the value of Δt is approximately equal to 2 ms, while for the largest admissible variations it may reach values of the order of 4 ms [2]. Thus, if we assume $\Delta t = 4$ ms, we may be sure that within this time interval we can move from any characteristic to any other one, regardless of the particular characteristics at hand.

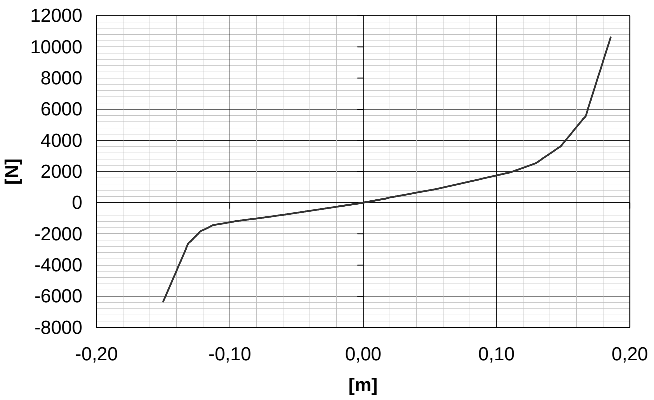

Figure 4: The nonlinear characteristic of the suspension spring.

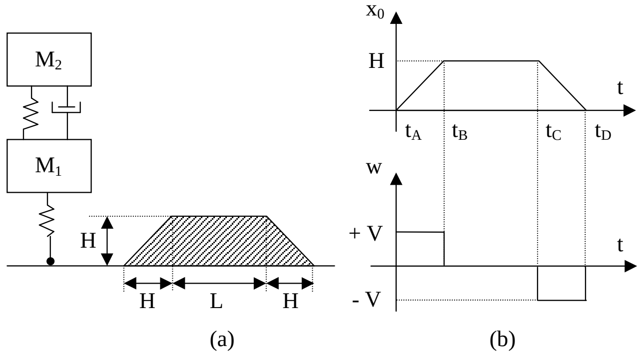

Figure 5: Geometrical characteristics of the bump (a) and the resulting disturbance $w(t) = \dot{x}_0(t)$ (b).

In previous works the delay time Δt has been neglected. This implies that, if at the generic time instant t we select a certain characteristic, then such a characteristic will only be reached at the time instant $t + \Delta t$, thus never allowing $u_s(\cdot)$ to be equal to $u_t(\cdot)$.

To overcome such a problem, in this paper our goal at time t becomes that of minimizing the quadratic difference among the semiactive control force and the target active control force at the time instant $t + \Delta t$, namely

$$(u_t(t + \Delta t) - u_s(t + \Delta t))^2.$$

The target control force has been chosen equal to

$$u_t(t + \Delta t) = -\boldsymbol{K}\hat{\boldsymbol{x}}(t + \Delta t).$$

The semiactive control force may be written as:

$$\begin{aligned} u_s(t + \Delta t) = \quad & -\lambda_s(x_1(t + \Delta t))x_1(t + \Delta t) - \\ & f(t + \Delta t)(x_2(t + \Delta t) - x_4(t + \Delta t)) \\ \simeq \quad & -\lambda_s(\hat{x}_1(t + \Delta t))\hat{x}_1(t + \Delta t) - F_d(t + \Delta t) \end{aligned}$$

where the $\hat{x}_i$ denotes the estimate of state x_i generated by the observer, while $F_d(t + \Delta t) = f(t + \Delta t)(\hat{x}_2(t + \Delta t) - \hat{x}_4(t + \Delta t))$ denotes the force due to the damper at the time instant $t + \Delta t$.

Thus, given the nonlinear characteristics of the damper, we restrict our attention to only those values of the force that can be generated when the suspension velocity deformation is equal to $\hat{x}_2(t + \Delta t) - \hat{x}_4(t + \Delta t) \simeq \dot{x}_1(t + \Delta t)$. We select the characteristic that generates the force that minimizes the quadratic difference:

$$(-\boldsymbol{K}\hat{\boldsymbol{x}}(t + \Delta t) + \lambda_s(\hat{x}_1(t + \Delta t))\hat{x}_1(t + \Delta t) + F_d(t + \Delta t))^2$$

and we denote it $F_d^*(t + \Delta t)$. Finally, we can impose the chosen characteristic selecting the corresponding value of the magnetization current.

5 Application example

In this section we discuss in detail the results of several simulations. First, however, we explain the choices we have made for the various parameters.

The proposed procedure has been applied to the quarter car suspension shown in Figure 1, with values of the parameters taken from [14]: $M_1 = 28.58$Kg, $M_2 = 288.90$Kg, $\lambda_t = 155900$N/m. In the simulation we used the non linear characteristic of the suspension spring suspension spring given in Figure 4. Finally, the characteristics of the damper [2] are those shown in Figure 3.

The matrices $\boldsymbol{Q}$ and r of the performance index J have been taken from [14] and are the same as those already used in [4, 6]: $\boldsymbol{Q} = diag\{1, 0, 10, 0\}, r = 0.8 \cdot 10^{-9}$. Thus, the resulting feedback control matrix is $\boldsymbol{K} = [35355 \; 4827 \; -21879 \; -1386]$. For the computation of the observer matrix we used the software tools available in Matlab: `fmins` is the minimization procedure and `normh2` computes the H_2 norm. We determined

$$\boldsymbol{K}_o = \begin{bmatrix} 176.1 & 1334.4 & 1.9 & -145.7 \\ 51.3 & 426.1 & 1852.5 & -5501.4 \end{bmatrix}^T.$$

Finally, we have taken $\Delta t = 0.4 \cdot 10^{-2}$s.

To show the performance of our semiactive suspension design, we have simulated two different situations.

5.1 Simulation 1

In the first simulation we consider null initial conditions, i.e., $\boldsymbol{x}(0) = \hat{\boldsymbol{x}}(0) = \boldsymbol{0}$ and assume that an external disturbance is acting on the system, caused by a bump in the road profile. The geometrical characteristics of the bump are shown in Figure 5.a.

We make the hypothesis that the velocity of the vehicle keeps at a constant value V during all time period of interest.

Moreover, we assume that the point of contact of the tire with the road perfectly follows the road profile, or equivalently we assume that no loss of contact between wheel and road may occur. Finally, we assume that the damping of the tire is negligible and its dynamical behaviour may be modelled through a pure elastic constant.

Under these hypothesis the vertical position x_0 of the point of contact of the tire with the road depends not only on the shape of the bump, but also on the velocity V of the vehicle. The value of x_0 wrt time t is shown in Figure 5.b where $(t_B - t_A) = (t_D - t_C) = H/V$. As a consequence, the external disturbance $w(t)$, i.e., the vertical velocity of the point of contact of the tire with the road, varies wrt time as shown in Figure 5.b.

The results of this simulation are shown in Figure 6, where we have taken $H = 25$ mm, $L = 50$ mm, and $V = 10$ m/s.

Figure 6.a shows the road profile x_0 (thin line) along with the unsprung mass displacement $x_3 + x_0$ (thick line). Figure 6.b

shows the road profile x_0 (thin line) along with the sprung mass displacement $x_1 + x_3 + x_0$ (thick line). It is possible to observe that the semiactive suspension well behaves in front of the abrupt obstacle, smoothing the movement of the sprung mass.

Figure 6.c compares the sprung mass displacement in the case of the semiactive suspension (thick line) and in the case of a completely passive suspension (thin line), while Figure 6.d compares the sprung mass displacement in the case of the semiactive suspension (thick line) and in the case of the target active suspension (thin line). As it can be noted, the behaviour of the semiactive suspension is intermediate between that of the passive and active suspension.

Figure 6.e compares the target force (thin line) with the control force produced by the semiactive suspension (thick line). We can observe that the variation of f guarantees a satisfactory approximation.

Figure 6.f shows the values of the index denoting the current nonlinear characteristic during the evolution of the semiactive suspension.

Figures 6.g – l show the efficiency of the asymptotic state observer used during simulations. We can observe that it provides a good evaluation of both the state variables and their derivatives. As an example, in Figure 6.g we have reported the evolution of the first state variable x_1, while in Figure 6.h we have reported the evolution of its error estimate $e_1 = x_1 - \hat{x}_1$. Figure 6.i shows the evolution of $\dot{x}_1$, while $\dot{e}_1 = \dot{x}_1 - \dot{\hat{x}}_1$ is reported in Figure 6.l.

5.2 Simulation 2

In the second simulation we consider an initial state different from zero and no external disturbance. We assume $\boldsymbol{x}(0) = [0.1\ 0\ 0.01\ 0]^T$. The results of this simulation are shown in Figure 7.

In the upper part, plots (a)-(b) compare the unsprung and the sprung mass displacement of the semiactive suspension with that of a completely passive suspension and a purely active one. Note that the spring of the passive suspension is the same as that used in the semiactive suspension, while the nonlinear characteristic of the damper is that one denoted with the number 7 in Figure 3. In particular, looking at plot (b) that shows the most significant variable, we can conclude that the semiactive system guarantees better performance than the passive one [4]. In fact, in such a case the behaviour of the semiactive suspension system in terms of the sprung mass displacement, is quite similar to that obtained using the purely active system.

The lower left plot (c) compares the target force with the control force produced by the semiactive suspension.

Finally, plot (d) shows the values of the index denoting the current nonlinear characteristic during the evolution of the semiactive suspension.

Remark 1. We observed that: (a) the prediction of the observer is always good for the given updating interval delay Δt; (b) during most of the time the active characteristic is the one labelled "1" in Figure 3. The first observation leads us to conclude that the updating frequency does not pose in practice any limitation. The second observation highlights the main drawback of this damper: even with a null magnetic field the damper coefficient is too high, and to improve the performance it should be necessary to have characteristic curves closer to the x axis than the one labelled "1".

6 Conclusions

This paper presents a two–phase design technique for magnetorheological semiactive suspensions.

The first phase of the project consists in the design of a target active control law that has been obtained by solving an LQR problem. The assumption of non-measurable state required the introduction of an asymptotic state observer, that has been designed using a procedure proposed by the authors in a previous work.

In the second phase, this target law is approximated by controlling the damper coefficient of the semiactive suspension. In particular, we have taken into account the delay Δt required for the updating of f: we have assumed that the new value of f is chosen so as to minimize the difference between the target and the semiactive control law at the time instant $t + \Delta t$. In such a way we can be sure that when the computed value of f is really imposed, then the semiactive force is as close as possible to the target one. The nonlinear behaviour of both the damper and the spring is also take into account to approximate the target active control law.

Several numerical simulations have been carried out considering a real existing MR damper.

References

[1] R. Caponetto, G. Fargione, A. Risitano, D. Tringali, "Soft computing for the design and optimization of a fuzzy sky-hook controller for semiactive suspensions," *XXX Convegno Nazionale AIAS* (Alghero, Italy), September 2001 (in Italian).

[2] Carrera web site, http://www.carreraschocks.com, 2002.

[3] G. Corriga, S. Sanna, G. Usai, "An optimal tandem active-passive suspension for road vehicles with minimum power consumption," *IEEE Trans. on Industrial Electronics*, Vol. 38, No. 3, pp. 210–216, 1991.

[4] G. Corriga, A. Giua, G. Usai, "An H_2 formulation for the design of a passive vibration–isolation system for cars," *Vehicle System Dinamics*, Vol. 26, pp. 381–393, 1996.

[5] M. Ebau, A. Giua, C. Seatzu, G.Usai, "Semiactive suspension design taking into account the actuator delay," *Proc. 40th IEEE Conference on Decision and Control* (Orlando, Florida), pp. 93–98, December 2001.

[6] A. Giua, C. Seatzu, G. Usai, "Semiactive suspension design with an optimal gain switching target," *Vehicle System Dinamics*, Vol. 31, pp. 213–232, 1999.

[7] E. Göring, E.C. von Glasner, R. Povel, P. Schützner, "Intelligent suspension systems for commercial vehicles," *Proc. Int. Cong. MV2, Active Control in Mechanical Engineering* (Lyon, France), pp. 1–12, June 1993.

[8] A. Hac, "Suspension optimisation of a 2-DOF vehicle model using a stochastic optimal control technique," *Journal of Sound and Vibration*, Vol. 100, No. 3, pp. 343–357, 1985.

[9] K.J. Kitching, D.J. Cole, D. Cebon, "Performance of semi-active damper for heavy vehicles," *ASME Journal of Dynamic Systems Measurement and Control*, Vol.122, pp.498-506, 2000.

[10] Lord Corporation web site, http://www.lord.com, 2002.

[11] M. Melas, "Nonlinear semiactive suspension design," *Laurea Thesis*, University of Cagliari, Italy, October 2002 (in Italian).

[12] K. Ogata, *Modern control engineering*, Prentice Hall International Editions, 1990.

[13] D. Sammier, "Modeling and control of suspension systems for road vehicle," *Ph.D. Thesis*, Lab. of Automatic Control of Grenoble, France, November 2001 (in French).

[14] A.G. Thompson, "An active suspension with optimal linear state feedback," *Vehicle System Dynamics*, Vol. 5, pp. 187–203, 1976.

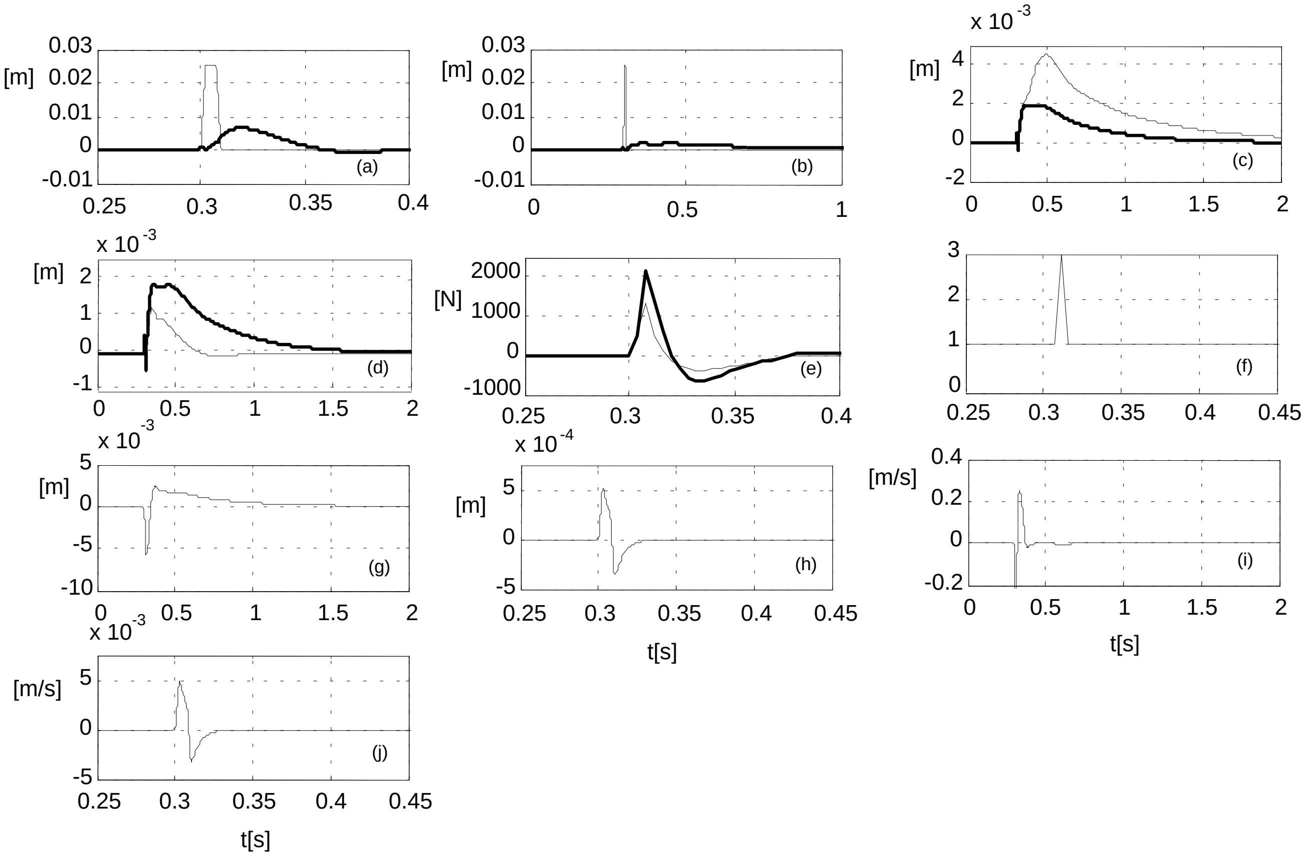

Figure 6: The results of Simulation 1.

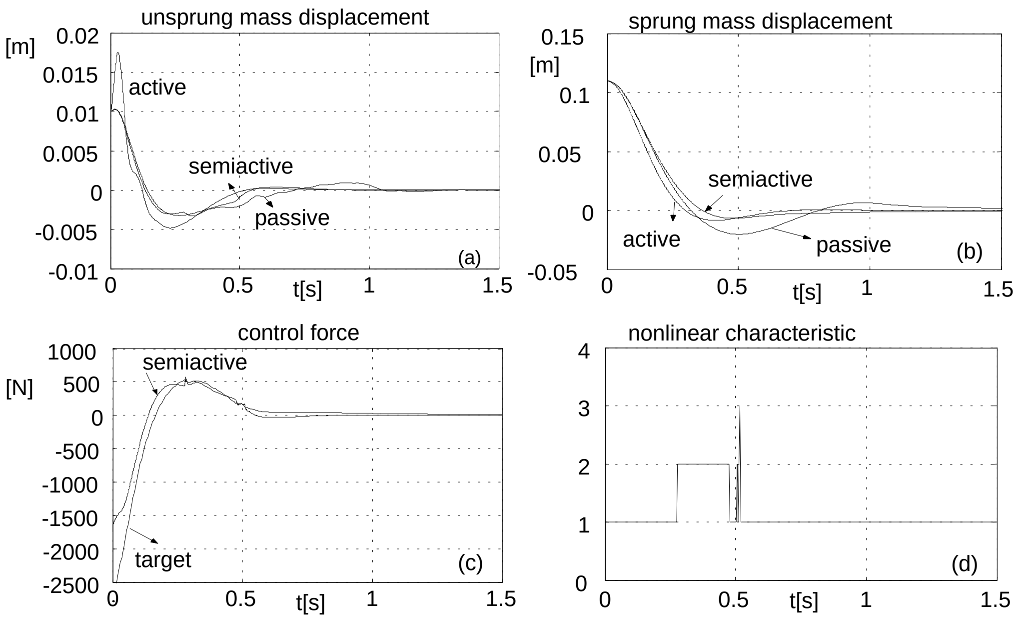

Figure 7: The results of simulation 2.